# Propagation of vortex electron wave functions in a magnetic field

Gregg M. Gallatin[*]

*National Institute of Standards and Technology Center for Nanoscale Science and Technology, Gaithersburg, Maryland 20899-6203, USA*

Ben McMorran

*Physics Department, University of Oregon, Eugene, Oregon 97403-1274, USA*

The physics of coherent beams of photons carrying axial orbital angular momentum (OAM) is well understood, and such beams, sometimes known as vortex beams, have found applications in optics and microscopy. Recently electron beams carrying very large values of axial OAM have been generated. In the absence of coupling to an external electromagnetic field, the propagation of such vortex electron beams is virtually identical mathematically to that of vortex photon beams propagating in a medium with a homogeneous index of refraction. But when coupled to an external electromagnetic field, the propagation of vortex electron beams is distinctly different from photons. Here we use the exact path integral solution to Schrodinger's equation to examine the time evolution of an electron wave function carrying axial OAM. Interestingly we find that the nonzero OAM wave function can be obtained from the zero OAM wave function, in the case considered here, simply by multiplying it by an appropriate time and position dependent prefactor. Hence adding OAM and propagating it can in this case be replaced by first propagating then adding OAM. Also, the results shown provide an explicit illustration of the fact that the gyromagnetic ratio for OAM is unity. We also propose a novel version of the Bohm-Aharonov effect using vortex electron beams.

## I. INTRODUCTION

Coherent beams of photons carrying axial orbital angular momentum (OAM), sometimes referred to as vortex beams, are well understood [1–3] and have various uses in optics and microscopy [4–7]. Recently electron beams carrying very high amounts of axial OAM have been generated [8] and the properties of such beams have been studied [9–12]. Mathematically the propagation of a vortex photon beam in a medium with a homogeneous index of refraction is virtually identical to that of a freely propagating vortex electron beam. This is obviously not the case when the electrons are propagating in an external electromagnetic field. Here we use the exact path integral solution to the full Hamiltonian, not the weak field approximation, to examine how an electron wave function carrying axial OAM evolves in time. We find that the propagation of a wave function carrying nonzero axial OAM is equivalent to the propagation of a zero OAM wave function multiplied by an appropriate position and time dependent prefactor. Also, the results provide an explicit illustration of the fact that the (nonradiatively corrected) gyromagnetic ratio for OAM is unity as it must be [12]. We will see that from a practical point of view this means that the OAM vector rotates at half the rate of the electron that circulates in a magnetic field, i.e., at half the cyclotron or Landau frequency.

The paper is organized as follows: Sec. II discusses the path integral solution for the (nonrelativistic) propagation of the electron wave function in a magnetic field. Section III uses the path integral solution to study how a vortex electron beam, actually a wave packet, evolves in a magnetic field and shows explicitly that the gyromagnetic ratio for OAM is unity.

## II. PATH INTEGRAL SOLUTION FOR PROPAGATION IN A MAGNETIC FIELD

One of the major early successes of the Dirac equation was that it automatically yielded (nonradiatively corrected) values for the gyromagnetic ratios of the orbital and spin angular momentum of an electron which matched experiment. Squaring the Dirac equation and extracting the nonrelativistic behavior yields an interaction term of the form $\vec{B} \cdot (\vec{\mathbf{L}} + 2\vec{\mathbf{S}})$, where $\vec{B}$ is a constant magnetic field, $\vec{\mathbf{L}}$ is the orbital angular momentum(OAM) operator, and $\vec{\mathbf{S}}$ is the spin angular momentum operator of the electron [13]. Thus OAM couples to the magnetic field as $\vec{B} \cdot \vec{\mathbf{L}}$, whereas the spin angular momentum couples as $2\vec{B} \cdot \vec{\mathbf{S}}$; thus the (nonradiatively corrected) gyromagnetic ratio for OAM is $g_L = 1$, whereas for spin angular momentum it is $g_S = 2$. This difference has the effect that whereas the spin of an electron projected in the direction of propagation, i.e., its helicity, remains tangent to the electron trajectory as it rotates in a magnetic field, but any axial OAM carried by the wave function does not; it will (up to radiative corrections) rotate at half the rate of the spin. It should be noted that $g_L = 1$ is a property of the Hamiltonian and not of the wave function and so must hold for all wave functions, even vortex wave functions. In spite of this it is still interesting and useful to show explicitly how the phase and amplitude of the wave function vary with time in order to achieve this.

We are interested in OAM and not spin, and so we consider the spinless Schrodinger equation

$$i\hbar \partial_t |\psi,t\rangle = \mathbf{H}|\psi,t\rangle, \tag{1}$$

*gregg.gallatin@nist.gov

with $\partial_t \equiv \partial/\partial t$. Here the Hamiltonian operator **H** is given by

$$\mathbf{H} = [\vec{\mathbf{P}} - e\vec{A}(\vec{\mathbf{R}})]^2/2m, \qquad (2)$$

with $\vec{\mathbf{P}}$ the momentum operator, $\vec{\mathbf{R}}$ the position operator, and $\vec{A}(\vec{x})$ the magnetic vector potential. In the position representation $\langle \vec{x}|\psi,t \rangle = \psi(\vec{x},t)$, to first order in the magnetic field, i.e., in the so-called "weak field approximation," this becomes

$$(i\hbar 2m\partial_t + \hbar^2\vec{\partial}^2 + e\vec{B} \cdot \vec{L})\psi(\vec{x},t) = 0, \qquad (3)$$

with $\vec{L} = -i\hbar\varepsilon_{ijk}\hat{x}_i x_j \partial_k$, where $\hat{x}_i$ is the unit vector in the $i$ direction and $\partial_i \equiv \partial/\partial x_i$. Unless otherwise stated the Einstein summation convention wherein repeated indices, $i, j, \ldots,$ are summed over the appropriate range will be used throughout.

Here we use the full Hamiltonian, (2), and not the weak field approximation, and so we need to solve

$$i\hbar\partial_t\psi(\vec{x},t) = \frac{1}{2m}[-i\hbar\vec{\partial} - e\vec{A}(\vec{x})]^2\psi(\vec{x},t) \qquad (4)$$

for a constant magnetic field.

Because (4) is linear and first order in the time derivative, the solution can be written in the form

$$\psi(\vec{x},t) = \int d^3x' K(\vec{x},t,\vec{x}',t')\psi(\vec{x}',t'), \qquad (5)$$

where $K(\vec{x},t,\vec{x}',t')$ is the so called "propagator" and the integral is nominally over all space. In addition, the fact that (4) is first order in time allows the propagator to be written as a path integral [13–15], i.e.,

$$K(\vec{x},t,\vec{x}',t') = \int_{(\vec{x}',t')}^{(\vec{x},t)} \delta\vec{x}(t) \exp\left[\frac{i}{\hbar}\int_{t_a}^{t_b} dt \mathcal{L}(\vec{x}(t),\partial_t\vec{x}(t),t)\right]. \qquad (6)$$

Here $\mathcal{L}(\vec{x}(t),\partial_t\vec{x}(t),t)$ is the classical Lagrangian corresponding to the quantum Hamiltonian (2), and the integral is over all paths or trajectories which go from $\vec{x}'$ at time $t'$ to $\vec{x}$ at time $t$. The Lagrangian corresponding to (2) has the form

$$\mathcal{L}(\vec{x}(t),\partial_t\vec{x}(t),t) = \tfrac{1}{2}m[\partial_t\vec{x}(t)]^2 - e\vec{A}(\vec{x}(t),t) \cdot \partial_t\vec{x}(t), \qquad (7)$$

where $\vec{A}$ is the vector potential with the magnetic field $\vec{B} = \vec{\partial} \times \vec{A}$. For a constant $\vec{B}$ field pointing in the 3 or $z$ direction, we can choose $A_1 = -\frac{1}{2}Bx_2, A_2 = \frac{1}{2}Bx_1,$ and $A_3 = 0$ or equivalently $A_x = -\frac{1}{2}By, A_y = \frac{1}{2}Bx,$ and $A_z = 0$. This gives

$$\mathcal{L}(\vec{x}(t),\partial_t\vec{x}(t)) = \frac{m}{2}[\partial_t\vec{x}(t)]^2 + \frac{eB}{2}\epsilon_{ij}x_i\partial_t x_j(t), \qquad (8)$$

where the subscripts $i, j$ are summed over the range 1,2 corresponding to the $x$ and $y$ directions, and $\epsilon_{ij}$ is defined by $\epsilon_{12} = -\epsilon_{21} = 1$ and $\epsilon_{11} = \epsilon_{22} = 0$. It should be noted that the Lagrangian in Eqs. (7) and (8) is the full Lagrangian, not the weak field approximation. This can be seen simply by calculating the corresponding classical Hamiltonian which is $H = (\vec{p} - e\vec{A})^2/2m$ with $\vec{p} = m\partial_t x(t)$.

The solution for the propagator with this Lagrangian is straightforward [14,15]; indeed it's given as a problem in Feynman *et al.*'s book [16]. Transform to a rotating frame

in the $x, y$ or 1,2 plane by writing

$$x_i = \exp\left[\frac{eBt}{2m}\epsilon\right]_{ij} X_j \Rightarrow \begin{pmatrix} x_1 \\ x_2 \end{pmatrix}$$

$$= \begin{pmatrix} \cos\left[\frac{eBt}{2m}\right] & \sin\left[\frac{eBt}{2m}\right] \\ -\sin\left[\frac{eBt}{2m}\right] & \cos\left[\frac{eBt}{2m}\right] \end{pmatrix} \begin{pmatrix} X_1 \\ X_2 \end{pmatrix}, \qquad (9)$$

where the matrix $\epsilon$ has elements $\epsilon_{ij}$. In terms of the new variables the Lagrangian corresponds to free propagation in the $z$ direction and a harmonic oscillator in the $X_i$, $i = 1,2$, directions with radian frequency $eB/2m$. The path integral solutions for free propagation and for a harmonic oscillator are well known [14,15]. Using these results and transforming back to the nonrotating coordinates, we get

$$K(\vec{x},t,\vec{x}',t')$$

$$= \left(\frac{m}{2\pi i\hbar T}\right)^{3/2} \frac{\frac{\omega}{2}T}{\sin\left[\frac{\omega}{2}T\right]} \exp\left[\frac{i}{2\hbar}\frac{m(z-z')^2}{T}\right.$$

$$\left. + \frac{m\omega}{2}\cot\left[\frac{\omega}{2}T\right](x_i - x_i')^2 + m\omega\epsilon_{ij}x_i x_j'\right], \qquad (10)$$

with

$$\omega = \frac{eB}{m}, \qquad (11)$$

which is the standard cyclotron frequency [15] and $T \equiv t - t'$. In Eq. (10) the combination $\omega T$ always occurs divided by 2, and so we should expect various aspects of the wave function to evolve at half the rate at which the electron circulates in the magnetic field.

Note that in the limit as $\omega \to 0$ the propagator in Eq. (10) reduces to the free propagator

$$K_{\text{free}}(\vec{r} - \vec{r}',t - t')$$

$$= \left(\frac{m}{2\pi i\hbar(t-t')}\right)^{3/2} \exp\left[\frac{im}{2\hbar}\frac{(x_i - x_i')^2}{t-t'}\right], \qquad (12)$$

which is explicitly space and time translation invariant as it should be.

## III. EVOLUTION OF A GAUSSIAN WAVE FUNCTION WITH AND WITHOUT OAM

The propagator given in Eq. (10) is Gaussian in form, and so if we choose a Gaussian for the wave function at $t' = 0$, it will remain Gaussian. Also, in this case the integral in Eq. (5) can be evaluated analytically.

First consider propagation perpendicular to the magnetic field. In this case let the initial normalized wave function be a Gaussian centered at the origin and propagating in the $x_2 = y$ direction:

$$\psi_0(\vec{r},0) = \frac{1}{\sqrt{\pi\sigma^2}\sqrt{\pi L^2}} \exp\left[-\frac{x^2 + z^2}{2\sigma^2} - \frac{y^2}{2L^2} + \frac{i}{\hbar}py\right], \qquad (13)$$

where we have switched from the $x_i$ notation to the more convenient at this stage $x, y, z$ notation with $\vec{r} = x\hat{x} + y\hat{y} + z\hat{z}$. This wave function is roughly $\sigma$ in width in the $x$ and $z$ directions and has length $L$ in the $y$ direction. If we specify the values of $\omega$ and the radius $R$ of the classical orbit of the electron, then $p = m\omega R$. If we take $\sigma$ and $L$ to be much larger than the nominal de Broglie wavelength of $2\pi\hbar/p$, then we expect mininal "diffraction" effects to occur during propagation and as shown explicitly below this is exactly the case. This initial wave function has zero OAM about it's direction of propagation, the $y$ direction, since

$$L_y \psi_0(\vec{r}, 0) = i\hbar(x\partial_z - z\partial_x)\psi_0(\vec{r}, 0) = 0. \quad (14)$$

To generate axial OAM we use the so-called ladder operator approach [17] which works as follows. Consider an operator **A** with eigenstate $|a\rangle$ such that $\mathbf{A}|a\rangle = a|a\rangle$. We now want to generate a state $|a+1\rangle$ such that $\mathbf{A}|a+1\rangle = (a+1)|a+1\rangle$. To do this we only need to find an operator **B** such that $[\mathbf{A}, \mathbf{B}] = \mathbf{B}$, since then $\mathbf{AB}|a\rangle = \mathbf{B}|a\rangle + \mathbf{BA}|a\rangle = (a+1)\mathbf{B}|a\rangle$ and so the state $\mathbf{B}|a\rangle = |a+1\rangle$, up to normalization and phase

factors. Noting that

$$[L_y/\hbar, (\partial_x - i\partial_z)] = [i(x\partial_z - z\partial_x), (\partial_x - i\partial_z)] = (\partial_x - i\partial_z),$$
$$(15)$$

it follows that a state with one unit of axial OAM, $\psi_1(\vec{r}, 0)$, is given (up to normalization and phase factors) by

$$\psi_1(\vec{r}, 0) = (\partial_x - i\partial_z)\psi_0(\vec{r}, 0)$$
$$= \frac{1}{\sigma^2}(-x + iz)\psi_0(\vec{r}, 0) = \frac{1}{\sigma^2}\rho e^{i\theta}\psi_0(\vec{r}, 0). \quad (16)$$

Here $\rho = \sqrt{x^2 + z^2}$ and $\theta$ increases in the counterclockwise direction when looking in the $-y$ direction and is measured from the $-x$ axis. Using the fact that $i(x\partial_z - z\partial_x) = -i\partial_\theta$, we immediately see that $L_y\psi_1 = \hbar\psi_1$ and so $\psi_1$ carries one unit of axial OAM. The factor of $\rho$, which appears automatically, is necessary since at $\rho = 0$ (=the $y$ axis in this case), the phase $\exp[i\theta]$ is not defined, and the wave function must vanish there. Note that operating on a Gaussian with powers of $(\partial_x \pm i\partial_z)$ yields the Laguerre-Gaussian functions [18].

Substituting $\psi_0(\vec{r}, 0)$ into (5) and using (10) gives

$$\psi_0(\vec{r}, t) = N \int d^3r' \exp\left[\frac{im}{2\hbar t}(z - z')^2 + \frac{im\omega}{4\hbar}\cot\left[\frac{\omega t}{2}\right][(x - x')^2 + (y - y')^2]\right.$$
$$\left. + \frac{im\omega}{2\hbar}(xy' - yx') - \frac{1}{2\sigma^2}(x'^2 + z'^2) - \frac{1}{2L^2}y'^2 + \frac{im\omega R}{\hbar}y'\right]$$
$$= N \exp\left[\frac{im}{2\hbar t}z^2 + \frac{im\omega}{4\hbar}\cot\left[\frac{\omega t}{2}\right](x^2 + y^2)\right] \int d^3r' \exp\left[\alpha_x x' + \alpha_y y' + \alpha_z z' - \frac{1}{2\beta_x}x'^2 - \frac{1}{2\beta_y}y'^2 - \frac{1}{2\beta_z}z'^2\right]$$
$$= N \exp\left[\frac{im}{2\hbar t}z^2 + \frac{im\omega}{4\hbar}\cot\left[\frac{\omega t}{2}\right](x^2 + y^2)\right] \sqrt{(2\pi)^3\beta_x\beta_y\beta_z} \exp\left[\frac{1}{2}\beta_x\alpha_x^2 + \frac{1}{2}\beta_y\alpha_y^2 + \frac{1}{2}\beta_z\alpha_z^2\right], \quad (17)$$

where

$$N = \left(\frac{m}{2\pi i\hbar t}\right)^{3/2} \frac{\frac{\omega t}{2}}{\sin\left[\frac{\omega t}{2}\right]} \frac{1}{\sqrt{\pi\sigma^2}\sqrt{\pi L^2}}, \quad \alpha_x = -\frac{im\omega}{2\hbar}\cot\left[\frac{\omega t}{2}\right]x - \frac{im\omega}{2\hbar}y, \quad \alpha_y = -\frac{im\omega}{2\hbar}\cot\left[\frac{\omega t}{2}\right]y + \frac{im\omega}{2\hbar}x + \frac{im\omega R}{\hbar},$$

$$\alpha_z = -\frac{im}{\hbar t}z, \quad \beta_x = \left(\frac{1}{\sigma^2} - \frac{im\omega}{2\hbar}\cot\left[\frac{\omega t}{2}\right]\right)^{-1}, \quad \beta_y = \left(\frac{1}{L^2} - \frac{im\omega}{2\hbar}\cot\left[\frac{\omega t}{2}\right]\right)^{-1}, \quad \beta_z = \left(\frac{1}{\sigma^2} - \frac{im}{\hbar t}\right). \quad (18)$$

To propagate $\psi_1$ we can write

$$\psi_1(\vec{r}, t) = N \int d^3r' K(\vec{r}, t, \vec{r}', 0)(\partial_{x'} - i\partial_{z'})\psi_0(\vec{r}', 0) = \frac{N}{\sigma^2} \int d^3r' K(\vec{r}, t, \vec{r}', 0)(-x' + iz')\psi_0(\vec{r}', 0)$$
$$= \frac{N}{\sigma^2}\partial_\lambda \int d^3r' K(\vec{r}, t, \vec{r}', 0) \exp[\lambda(-x' + iz')]\psi_0(\vec{r}', 0)|_{\lambda=0}. \quad (19)$$

The integral is still Gaussian and can be evaluated as above by letting $\alpha_x \to \alpha_x - \lambda$ and $\alpha_z \to \alpha_z + i\lambda$ in Eq. (17). Taking the derivative with respect to $\lambda$ and setting $\lambda = 0$ then yields

$$\psi_1(\vec{r}, t) = \frac{N}{\sigma^2} \exp\left\{\frac{im}{2\hbar t}z^2 + \frac{im\omega}{4\hbar}\cot\left[\frac{\omega t}{2}\right](x^2 + y^2)\right\} \sqrt{(2\pi)^3\beta_x\beta_y\beta_z}(-\beta_x\alpha_x + i\beta_z\alpha_z) \exp\left[\frac{1}{2}\beta_x\alpha_x^2 + \frac{1}{2}\beta_y\alpha_y^2 + \frac{1}{2}\beta_z\alpha_z^2\right]$$
$$= (-\beta_x\alpha_x + i\beta_z\alpha_z)\frac{1}{\sigma^2}\psi_0(\vec{r}, t), \quad (20)$$

with $\alpha_x, \beta_x, \ldots$ the same as in Eq. (18).

Even though both these analytic solutions can be manipulated into somewhat more convenient forms, this is not very illuminating, and so we will simply plot these solutions for a set of conditions which nicely illustrate the relevant aspects of their

time evolution. On the other hand it is worthwhile to examine the factor $(-\beta_x\alpha_x + i\beta_z\alpha_z)$ to get a better understanding of how it evolves and controls the orientation of the OAM. Substituting from above we find, after some algebra,

$$f(\vec{r},t) \equiv -\beta_x\alpha_x + i\beta_z\alpha_z = \frac{\cos\left[\frac{\omega t}{2}\right]x + \sin\left[\frac{\omega t}{2}\right]y}{\left(\sin\left[\frac{\omega t}{2}\right]\frac{2\hbar}{im\omega\sigma^2} - \cos\left[\frac{\omega t}{2}\right]\right)} + i\frac{z}{\left(1 - \frac{\hbar t}{im\sigma^2}\right)}. \tag{21}$$

We see that $f(\vec{r},0) = -x + iz$ at $t = 0$, as it should, and that it rotates in time in the $xy$ plane at a radian frequency of $\omega/2$. The origin of this factor is obvious. In operator notation, ignoring the $1/\sigma^2$, (16) becomes

$$|\psi_1\rangle = (-\mathbf{X} + i\mathbf{Z})|\psi_0\rangle. \tag{22}$$

The time evolution is given by

$$e^{-i\mathbf{H}t/\hbar}|\psi_1\rangle = e^{-i\mathbf{H}t/\hbar}(-\mathbf{X} + i\mathbf{Z})|\psi_0\rangle = [e^{-i\mathbf{H}t/\hbar}(-\mathbf{X} + i\mathbf{Z})e^{+i\mathbf{H}t/\hbar}]e^{-i\mathbf{H}t/\hbar}|\psi_0\rangle = f(\vec{\mathbf{R}},t)e^{-i\mathbf{H}t/\hbar}|\psi_0\rangle, \tag{23}$$

where $\mathbf{H} = [\vec{\mathbf{P}} - e\vec{A}(\vec{\mathbf{R}})]^2/2m$ is the quantum Hamiltonian corresponding to the Lagrangian (8).

The position of the node of $\psi_1(\vec{r},t)$ follows from the solution to $f(\vec{r},t) = 0$. At $t = 0$ this is the $y$ axis as shown above. For arbitrary $t$ we have the solution

$$y = -\cot\left[\frac{\omega t}{2}\right]x, \quad z = 0. \tag{24}$$

This solution is illustrated in Fig. 1 for several values of $t$. This "nodal line" rotates only by $\pi$ during one full period, $\tau = 2\pi/\omega$, of the electron cyclotron orbit, and since this factor is the origin of the OAM carried by $\psi_1$, this shows explicitly that the OAM rotates at half the cyclotron frequency, i.e., $g_L = 1$. This also shows that the OAM is axially oriented only at times $t = n\tau$, with $n = 0,1,2,\ldots$, and its direction switches between being parallel and antiparallel to the direction of propagation at each of these times.

Note that $\psi_0(\vec{r},t)$ and $\psi_1(\vec{r},t)$ are not simply propagating Gaussian envelope functions multiplied by a propagating plane wave factor of the form $\exp[i\vec{p}\cdot\vec{r}/\hbar - iEt/\hbar]$ with $|\vec{p}|$ constant (but rotating at radian frequency $\omega$) and

$E = |\vec{p}|^2/2m$. For both wave functions the de Broglie wavelength varies in time. This is to be expected since the coupling to the vector potential contributes an extra phase, the so-called "Dirac phase" [19] to the wave function of the form $-i/\hbar\int_0^t dt\,\vec{A}(\vec{r})\cdot\partial_t\vec{r}(t)$ which varies with position in generally a nonlinear fashion. Figures 2 and 3 show slices of the modulus squared and the real parts of $\psi_0$ and $\psi_1$ in the $xy$ plane at different positions in the orbit. The values chosen for $\sigma, L, \omega$, and $R$ are such that the size of the wave packet at $t = 0$ ($L$ in the $y$ direction and $\sigma$ in the $x$ direction) is both much larger
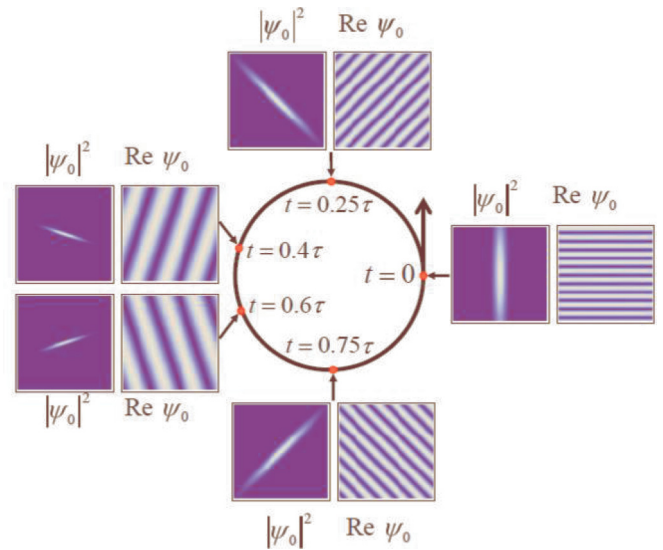


FIG. 2. (Color online) Slices in the $xy$ plane of $|\psi_0|^2$ and $\text{Re}[\psi_0]$ at different positions around the cyclotron orbit where $\psi_0$ is a Gaussian wave packet carrying 0 axial orbital angular momentum (OAM). The values chosen for the width $\sigma$ and length $L$ of the wave packet, the cyclotron frequency $\omega = eB/m$, and the radius of the cyclotron orbit $R$ are such that the size of the wave packet at $t = 0$ ($L$ in the $y$ direction and $\sigma$ in the $x$ direction) is much larger than the wavelength so that diffraction effects are minimal. All the plots are the same fixed spatial scale with that of the $\text{Re}[\psi_0]$ plots being about five orders of magnitude smaller than the $|\psi_0|^2$ plots so that the phase of the wave packet is visible. At $t = 0.5\tau$ the wave packet would be too small to be seen at this fixed spatial scale, and so it is shown at times $t = 0.4\tau$ and $t = 0.6\tau$ instead.



FIG. 1. (Color online) The graph shows the nodal lines (dashed) at different positions in the electron orbit. The OAM lies along the nodal lines, and thus rotates at $\omega = eB/2m$ which is half the cyclotron frequency.
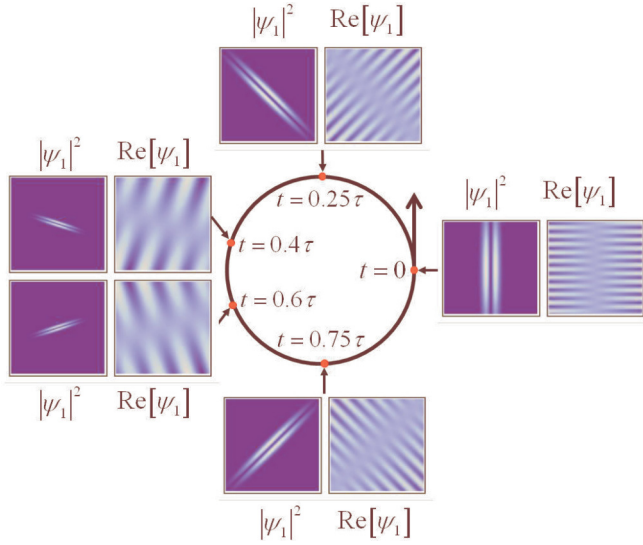
FIG. 3. (Color online) Slices in the $xy$ plane of $|\psi_1|^2$ and $\text{Re}[\psi_1]$ at different positions around the cyclotron orbit where $\psi_1$ is a Laguerre-Gaussian wave packet carrying one unit of axial orbital angular momentum (OAM) oriented in the $y$ direction at $t = 0$. The values chosen for the width $\sigma$ and length $L$ of the wave packet, the cyclotron frequency $\omega = eB/m$, and the radius of the cyclotron orbit $R$ are the same as in Fig. 2, i.e., they are such that the size of the wave packet at $t = 0$ ($L$ in the $y$ direction and $\sigma$ in the $x$ direction) is much larger than the wavelength so that diffraction effects are minimal. All the plots are the same fixed spatial scale with that of the $\text{Re}[\psi_1]$ plots being about five orders of magnitude smaller than the $|\psi_1|^2$ plots so that the phase of the wave packet is visible. At $t = 0.5\tau$ the wave packet would be too small to be seen at this fixed spatial scale, and so it is shown at times $t = 0.4\tau$ and $t = 0.6\tau$ instead.

than the wavelength (so that diffraction effects are minimal) and $R$ is much larger than $L$. The actual ratios used for the plots are $R = 10^3 L, L = 10\sigma$, and $\sigma \simeq 10^5 2\pi\hbar/m\omega$; hence the spatial range of the $\text{Re}[\psi_0]$ and $\text{Re}[\psi_1]$ plots is about five orders of magnitude smaller than for the $|\psi_0|^2$ and $|\psi_1^2|$ plots so that the phase variation is visible.

In Fig. 2 we see that the long axis of the wave function and the normals to the wavefronts of the wave function both track the nodal line in Fig. 1. Hence the wave function is rotating about its center of mass with the Larmor frequency $\omega/2$. As mentioned above, this is because $\omega T$ always occurs as $\omega T/2$ inside trigonometric functions in the propagator (10), and so we should expect the periodicity of certain aspects of the wave function to evolve at $\omega/2$ rather than $\omega$. The spatial extent of the wave function varies with period $\tau$, and thus the length and width return, up to diffraction effects, to their initial values at every $t = \tau, 2\tau, 3\tau, \ldots$. This periodic variation in the spatial extent of the wave function can be traced back to the fact that in the rotating frame the Lagrangian is that of a harmonic oscillator. The free propagation part of the Lagrangian, $m(\partial_t x)^2/2$, causes the wave function to expand or diffract as it propagates [20]. The harmonic oscillator part, $m\omega^2 \vec{x}^2/2$, causes the wave function to contract, and unless these two effects are precisely balanced the wave function will oscillate in size. This is exactly analogous to the propagation of a paraxial Laguerre-Gaussian photon beam centered on the

$z$ axis and propagating in the $z$ direction in a medium with an index of refraction of the form $n(x,y) = n_0 - c(x^2 + y^2)$, i.e, a harmonic oscillator potential, such as that of a parabolic graded index (GRIN) multimode fiber [21,22]. In the paraxial approximation the propagator for the photon beam in this case has the same Gaussian form as the propagator for the harmonic oscillator. The quadratic variation of the index of refraction will case the beam to focus or shrink in size as it propagates whereas diffraction effects cause the beam to expand as it propagates. If the beam is large, so that the focusing effect dominates, then the beam will shrink in size as it propagates. Eventually it shrinks to where the diffraction effect dominates and it begins to expand. This process repeats itself causing the beam to oscillate in size with a fixed period along its length. These oscillations can be prevented if the size of the beam is fine tuned so that the diffraction and focusing effects exactly cancel [21,22].

Figure 3 shows the propagation of the wave function $\psi_1$ carrying a single unit of OAM. The node in the center of the wave function maintains its alignment on the nodal line during each cycle. The spiral form of the phase of $\psi_1$ is apparent in the $\text{Re}[\psi_1]$ plots. Clearly the OAM is rotating at half the cyclotron frequency $\omega$. Note that this is also predicted by a semiclassical model of the orbital magnetic moment of an electron vortex wave function undergoing Larmor precession in an external field. A free electron with quantized OAM $L_y$ possesses an associated magnetic dipole $\mu = g_L\mu_B L_y/\hbar$, where $\mu_B$ is the Bohr magneton [9]. With $g_L = 1$, the state will precess at Larmor frequency $eB/2m$, half the cyclotron frequency. We thus find that the electron vortex beam helicity, defined as $\vec{L} \cdot \vec{p} / |\vec{p}|$, is not generally conserved in transverse magnetic fields, which may have implications for the validity of the model developed in Ref. [9]. The Larmor frequency of the electron's *spin* is, up to radiative corrections, equal to the cyclotron frequency. Thus, after rotating by $2\pi$, the spinor component of the wave function has rotated approximately by $2\pi$, but the complex amplitude of the wave function has rotated only by $\pi$

Although it might be possible to interpret the $\pi$ phase change of the OAM in one cycle as yet another case of Berry's geometric phase [23], it seems more natural to consider it as a dynamic rather than a geometric effect. Indeed, the classical equation for motion in the plane, $m\partial_t^2 x_i = (eB/m)\epsilon_{ij}\partial_t x_j$ with $i, j = 1,2$, can be interpreted as a precession equation for both the position vector $x_i$ and the momentum vector $p_i = m\partial_t x_i$ with both vectors precessing at $\omega = eB/m$. A complete cycle is defined by the position and momentum vectors both rotating by $2\pi$, and hence the angular momentum will rotate only by $\pi$ in a complete cycle. Finally since we are doing a purely nonrelativisitic calculation, Thomas precession, which is the first order, i.e., $v/c$, relativistic correction to the nonrelativistic result, is not accounted for in our analysis.

Now consider propagation parallel to the magnetic field. In this case we let

$$\psi_0(\vec{r},0) = \frac{1}{\sqrt{\pi\sigma^2}\sqrt{\pi L^2}} \exp\left[-\frac{x^2 + y^2}{2\sigma^2} - \frac{z^2}{2L^2} + \frac{i}{\hbar}pz\right]$$

$$(25)$$

and

$$\psi_0(\vec{r},t) = N \int d^3r' \exp\left[\frac{im}{2\hbar t}(z-z')^2 + \frac{im\omega}{4\hbar}\cot\left[\frac{\omega t}{2}\right][(x-x')^2 + (y-y')^2]\right.$$

$$\left. + \frac{im\omega}{2\hbar}(xy' - yx') - \frac{1}{2\sigma^2}(x'^2 + y'^2) - \frac{1}{2L^2}z'^2 + \frac{ip}{\hbar}z'\right]$$

$$= N\exp\left\{\frac{im}{2\hbar t}z^2 + \frac{im\omega}{4\hbar}\cot\left[\frac{\omega t}{2}\right](x^2 + y^2)\right\} \int d^3r' \exp\left[\alpha_x x' + \alpha_y y' + \alpha_z z' - \frac{1}{2\beta_\rho}(x'^2 + y'^2) - \frac{1}{2\beta_z}z'^2\right]$$

$$= N\sqrt{(2\pi)^3\beta_\rho^2\beta_z}\exp\left\{\left[\frac{im\omega}{4\hbar}\cot\left[\frac{\omega t}{2}\right] - \frac{1}{2}\beta_\rho\left(\frac{m\omega}{2\hbar\sin\left[\frac{\omega t}{2}\right]}\right)^2\right](x^2 + y^2) - \beta_z\left(\frac{m}{\hbar t}\right)^2\left(z - \frac{p}{m}t\right)^2 + \frac{im}{2\hbar t}z^2\right\}, \quad (26)$$

where $N$ is the same as in Eq. (18) but now

$$\beta_\rho = \left(\frac{1}{\sigma^2} - \frac{im\omega}{2\hbar}\cot\left[\frac{\omega t}{2}\right]\right)^{-1}, \quad \beta_z = \left(\frac{1}{L^2} - \frac{im}{\hbar t}\right). \quad (27)$$

Because $\psi(\vec{r},t)$ depends on $x$ and $y$ only in the combination $\rho^2 = x^2 + y^2$, it follows that the initial Gaussian wave function chosen here does not pick up angular momentum as it propagates along the magnetic field. In fact for propagation parallel to the magnetic field, the axial OAM of an eigenstate of $\mathbf{L}_z$ is conserved. This follows directly from

$$[\mathbf{L}_z, \mathbf{H}] = 0, \quad (28)$$

where again $\mathbf{H} = [\vec{\mathbf{P}} - e\vec{A}(\vec{\mathbf{R}})]^2/2m$ and $\mathbf{A}_i = -\frac{B}{2}\epsilon_{ij}\mathbf{X}_j$. Indeed it can be shown that $\mathbf{H} = \frac{1}{2m}\vec{\mathbf{P}}^2 - \frac{eB}{2m}\mathbf{L}_z + \frac{e^2B^2}{2m}(\mathbf{X}^2 + \mathbf{Y}^2)$ which obviously yields (28).

## IV. CONCLUSION

Using the exact path integral solution for the propagator in a constant magnetic field, we have derived the evolution of a Laguerre-Gaussian electron vortex wave function and shown explicitly that the (nonradiatively corrected) gyromagnetic ratio $g_L$ for OAM is unity. This must be the case since $g_L$ is a property of the Hamiltonian and not of the wave function. In a transverse magnetic field, we find that the wave function rotates $180°$ in a full cyclotron orbit, and this corresponds to Larmor precession of the electron vortex orbital magnetic moment rotating at half the cyclotron frequency. We also find that the wave function, with or without OAM, expands and contracts along the cyclotron trajectory. In a longitudinal magnetic field, we find that the axial OAM is conserved since $\mathbf{L}_z$ commutes with the Hamiltonian.

The results presented above can also be extended to present a novel version of the Aharonov-Bohm effect [24]. Consider a long thin solenoid aligned along the $z$ axis. Outside the solenoid (far from the ends), $\vec{A}$ varies as $1/\rho = 1/\sqrt{x^2 + y^2}$ and so $\vec{B}$ is zero outside. Inside the solenoid $\vec{A}$ varies as $\rho$ and so $\vec{B}$ is constant and nonzero, but a Laguerre-Gaussian wave function carrying nonzero OAM propagating along the $z$ axis has a node at the position of the solenoid. In fact, wave functions carrying large values of OAM have a very large region around the $z$ axis where the wave function is effectively zero [8]. As in the standard Aharonov-Bohm experiment [24] this is a case where there is no overlap between the wave function and the magnetic field. The wave function only overlaps with the magnetic vector potential. Hence the presence of the solenoid will cause a change in how the wave function propagates relative to the no solenoid case. This effect will predominantly result in a change in the focus position of the wave function. Experimental verification of this would provide yet another example of the fact $A_\mu$ is the fundamental quantity and not $\vec{E}$ and $\vec{B}$.

[1] Mark R. Dennis, Kevin O'Holleran, and Miles J. Padgett, Prog. Opt. **53**, 293 (2009).

[2] Miles Padgett, Johannes Courtial, and Les Allen, Phys. Today **57**(5), 35 (2004).

[3] U. D. Jentschura and V. G. Serbo, Phys. Rev. Lett. **106**, 013001 (2011).

[4] Sri Rama Prasanna Pavani and Rafael Peistun, Opt. Exp. **16**, 3484 (2008).

[5] Gabriel Molina-Terriza, Juan P. Torres, and Lluis Torner, Nat. Phys. **3**, 305 (2007).

[6] Sri Rama Prasanna Pavani, Michael A. Thompson, Julie S. Biteen, Samuel J. Lord, Na Liu, Robert J. Twieg, Rafael Piestun, and W. E. Moerner, Proc. Natl. Acad. Sci. USA **106**, 2995 (2009).

[7] Michael A. Thompson, Matthew D. Lew, Majid Badieirostami, and W. E. Moerner, Nano Lett. **10**, 211 (2010).

[8] Benjamin J. McMorran, Amit Agrawal, Ian M. Anderson, Andrew A. Herzing, Henri J. Lezec, Jabez J. McClelland, and John Unguris, Science **331**, 192 (2011).

[9] Konstantin Yu. Bliokh *et al.*, Phys. Rev. Lett. **99**, 190404 (2007).

[10] J. Verbeek, H. Tian, and P. Schattschneider, Nature (London) **467**, 301 (2010).

[11] P. Schattschneider and J. Verbeeck, Ultramicroscopy **111**, 1461 (2011).

[12] Konstantin Yu. Bliokh, Mark R. Dennis, and Franco Nori, Phys. Rev. Lett. **107**, 174802 (2011).

[13] A. Zee, *Quantum Field Theory in a Nutshell*, 2nd ed., Chap. III.6 (Princeton University Press, Princeton, 2010).

[14] Richard P. Feynman, Albert R. Hibbs, and Daniel F. Styer, *Quantum Mechanics and Path Integrals: Emended Edition*, (Dover Publications, Mineola, NY, 2010).

[15] Hagen Kleinert, *Path Integrals in Quantum Mechanics, Statistics, Polymer Physics, and Financial Markets*, 5th ed., Chap. 2.18 (World Scientific Publishing Company, Singapore, 2009).

[16] Richard P. Feynman, Albert R. Hibbs, and Daniel F. Styer, *Quantum Mechanics and Path Integrals: Emended Edition*, Problem 3–10 (Dover Publications, Mineola, NY, 2010).

[17] See, for example, J. J. Sakurai and Jim J. Napolitano, *Modern Quantum Mechanics*, 2nd ed. (Addison Wesley, London, 2011).

[18] Francesco Pampaloni and Joerg Enderlein, arXiv:physics/0410021v1.

[19] M. V. Berry, Eur. J. Phys. **1**, 240 (1980).

[20] H. Y. Kim and J. H. Weiner, Phys. Rev. B **7**, 1353 (1973).

[21] M. D. Feit and J. A. Fleck Jr., Appl. Opt. **17**, 3990 (1978).

[22] See, for example, Amnon Yariv and Pochi Yeh, *Optical Waves in Crystals: Propagation and Control of Laser Radiation*, Chap. 2 (Wiley-Interscience, Hoboken, 2002).

[23] M. V. Berry, Physics Today **43**(12), 34 (1990).

[24] See, for example, A. Zee, *Quantum Field Theory in a Nutshell*, 2nd ed., Chap. IV.4 (Princeton University Press, Princeton, 2010).